A molecular dynamics study of the thermal properties of thorium oxide

Paul Martin, David J. Cooke, and Robert Cywinski

Related Articles

Residual stresses and clamped thermal expansion in LiNbO3 and LiTaO3 thin films
Appl. Phys. Lett. 101, 122902 (2012)

Three-axis correction of distortion due to positional drift in scanning probe microscopy
Rev. Sci. Instrum. 83, 083711 (2012)

Anomalous thermal expansion of Sb2Te3 topological insulator
Appl. Phys. Lett. 100, 251912 (2012)

Multiferroic bending mode resonators and studies on temperature dependence of magnetoelectric interactions
Appl. Phys. Lett. 100, 242902 (2012)

The specific heat and the radial thermal expansion of bundles of single-walled carbon nanotubes
Low Temp. Phys. 38, 523 (2012)

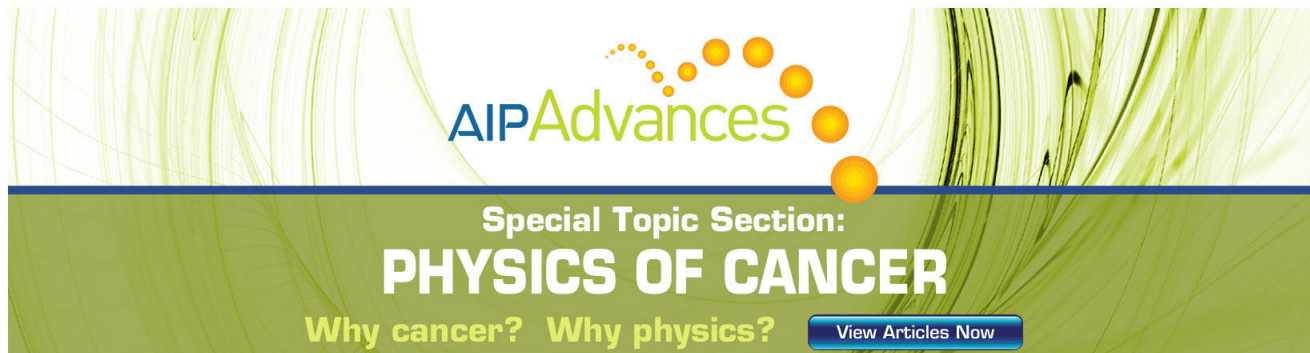## Additional information on J. Appl. Phys.

Journal Homepage: http://jap.aip.org/

Journal Information: http://jap.aip.org/about/about_the_journal

Top downloads: http://jap.aip.org/features/most_downloaded

Information for Authors: http://jap.aip.org/authors

A molecular dynamics study of the thermal properties of thorium oxide

Paul Martin, David J. Cooke,[a)] and Robert Cywinski
School of Applied Sciences University of Huddersfield, Huddersfield, United Kingdom

There is growing interest in the exploitation of the thorium nuclear fuel cycle as an alternative to that of uranium. As part of a wider study of the suitability of thorium dioxide (thoria) as a nuclear fuel, we have used molecular dynamics to investigate the thermal expansion, oxygen diffusion, and heat capacity of pure thoria and uranium doped (1-10%) thoria between 1500 K and 3600 K. Our results indicate that the thermal performance of the thoria matrix, even when doped with 10%U, is comparable to, and possibly better than, that of UO_2. © 2012 American Institute of Physics. [http://dx.doi.org/10.1063/1.4754430]

I. INTRODUCTION

Although thorium is fertile rather than fissile it has the potential to be an extremely important nuclear fuel.[1] Thorium is four times more plentiful in the earth's crust than uranium, the current fuel of choice and, moreover, it does not need isotopic enrichment before deployment. Consequently, there is, globally, sufficient thorium to provide the world's energy needs for several thousand years. Thorium has the additional advantage of generating significantly less waste, in the form of plutonium and the higher actinides, than uranium. Indeed, legacy waste can be mixed with thorium and transmuted, with significant reduction of its radiotoxicity.[2]

Historically, thorium nuclear fuel has played a role in power generation, but over the last four decades, the nuclear industry has focussed almost entirely on the uranium/plutonium fuel cycles. Nevertheless, there is currently a growing global interest in revisiting thorium as a potential safer and more sustainable fuel. Therefore, considerable attention is being devoted to developing, for example, the thorium molten salt reactor (MSR), thorium/uranium or thorium/plutonium fuel for conventional pressurised water reactors (PWR) and advanced heavy water reactors (AHWR), as well as the thorium fuelled accelerator driven subcritical reactor (ADSR) or energy amplifier. The AHWR system, fuelled by thorium/plutonium mixed oxide, is being actively pursued in India as a method of exploiting the indigenous thorium reserves. Whilst the ADSR systems, which exploit proton driven spallation from a heavy metal target within the reactor core to produce the neutrons necessary to induce fertile to fissile conversion within the thorium fuel and to sustain the fission process, are still under development.

The thorium fuel in both ADSR and the more conventional reactor systems is likely to take the form of thorium dioxide (or thoria) or mixed thoria/uranium oxide and thoria/plutonium oxides. In such fuel, the fertile ^{232}Th is converted into fissile ^{233}U with the fuel elements remaining within the reactor cores for years rather than months, as is the case with conventional uranium fuel. A full understanding of the material properties of thoria and its performance in intense radiation fields is therefore essential. However, on the one hand, detailed experimental analysis of thoria and uranium doped thoria under operating conditions is generally difficult, whilst on the other there have been very few atomistic studies on modelling the properties of thoria, particularly in the presence of uranium. In an attempt to redress this problem, we have carried out a detailed molecular dynamics study of the thermal properties of thorium oxide.

II. THEORY AND METHODOLOGY

Our simulations are based on the Born model of the ionic solid,[3] where the ions within the system are considered to be a series of charged interacting particles. These interactions are dominated by the long range Coulombic terms; which are solved using Ewald summation.[4] Shorter ranged Van der Waals interactions and electron-electron repulsions are incorporated into the model using pair-wise, parameterised potentials such as Buckingham and Lennard-Jones potentials, which are derived from pre-existing experimental data or from *ab initio* calculations. The potential parameters used in this work are from the rigid ion potentials first derived by Lewis and Catlow[5] and were chosen because they have previously been used successfully to model a range of oxides with the fluorite structure such as UO_2, ZrO_2, and CeO_2[6–10] and because parameters for uranium ions are also included in the potential set.

The parameters were derived empirically and tested against experimental structures, lattice parameters, elastic and dielectric constants. In their derivation, the authors assumed that all cation–cation interactions are purely coulombic and that the attractive r^{-6} term of the cation–anion interaction is zero (the interaction is essentially a Born-Meyer potential) as the small contribution of such terms to the short-range potential at the lattice inter-atomic spacing was instead incorporated by modification of the other parameters in the model.

Here, we also note that potential parameters, both fitted by Lewis and Catlow[5] and others,[11] and incorporating the shell model of Dick and Overhauser[12] are available and would add a level of polarisability to the model. However, this comes at a cost, first because the number of atoms is effectively doubled within each simulation and also, because

a)E-mail: d.j.cooke@hud.ac.uk.

112, 073507-1

of the small masses associated with the shells when using the adiabatic model within molecular dynamics simulations,[13] consequently, the time step must also be reduced by as much as a factor of ten, increasing the computational cost of the simulations. Trial simulations, conducted with rigid ion and shell models showed a little difference in the ability of the models to reproduce the bulk crystal. As discussed in more detail in Sec. III A, the rigid ion potential reproduces the crystal structure of thoria to within 1% of experiment across the temperature range considered in this study. A more detailed survey of available urania potentials[14,15] also concluded that there was a little difference between results from rigid ion and more complex potentials and thus the results reported here are based on a rigid ion potential and the parameters are shown in Table I.

A. Molecular dynamics

In order to determine the structural and thermodynamic properties of thoria, a series of molecular dynamics simulations have been performed using the DL_POLY 2 code.[16] All the simulations were performed using the Isotension-Isothermal Ensemble, constant number of particles, stress and temperature (NσT). This allows the size and the shape of the simulation cell to change during the simulations. The constant temperature and stress were maintained by applying Nosé–Hoover thermostats and barastats[17,18] both with a relaxation time (period) of 1.0 ps. When considering pure, bulk ThO$_2$, a $5 \times 5 \times 5$ super cell, containing 500 formula units was used within periodic boundary conditions. This ensured that the lattice energy of the system had converged and also gave sufficient cation sites for defects to be introduced into the system at the required concentrations. The time step used in all the simulations was 1 fs and the total simulation time was 1.1 ns of which temperature scaling was applied for the first 0.1 ns. A short range cut-off of 10 Å was applied throughout.

The simulations were run over a temperature range between 1500 K and 3600 K. At each temperature, five simulations were performed for a pure thoria cell, and four substituted cells in which the level of uranium doping ranged from 1% to 10%. Additionally, as it is unlikely that at these temperatures the crystal will be stoichiometrically pure, simulations were run with oxygen interstitials and oxygen vacancies present in the pure crystal. The presence of such defects also represents a first step to investigating the effect of radiation damage on the system. The vacancies and interstitials were added by randomly selecting the required number of lattice sites in the $5 \times 5 \times 5$ super cell, substituting a uranium atom for a thorium atom, and either removing a lattice oxygen or placing an oxygen on a previously vacant octahedral site.

In the systems where oxygen defects have been included charge neutrality was maintained by adjusting the charge of the dopant uranium ions. However, in doing so, we have assumed that the short range U–O interactions remain constant and hence the original parameters of Lewis and Catlow are used to describe all such interactions. This assumption is justified because as previously noted, the interactions in an ionic system are dominated by the coulombic interactions with the short-range potential essentially providing a repulsive wall at small ion separations. Whilst this would not be the best approach to follow if we were studying solid U$_2$O$_5$, where fitting a new U^{5+}–O interaction would be required, our model does reproduce the experimental lattice parameters to within 10% of experiment. Thus, as we are dealing with a small number of dopant ions in a system that remains essentially in the ThO$_2$, fluorite, structure, the assumption is more appropriate.

III. RESULTS AND DISCUSSION

It is clear that a nuclear fuel's performance will be affected by the thermophysical properties of the material being used. ThO$_2$ has previously been reported as having a higher thermal conductivity and lower co-efficient of thermal expansion when compared to UO$_2$,[19] suggesting it is a suitable candidate as an alternative nuclear fuel. However, as thorium itself is not fissile and therefore the nuclear energy is still produced from the fission of uranium (either U-233 from the decay of Th-233 or U-235 from doping the fuel rod), many important questions relate to how these favourable properties may be affected by such uranium at operational temperatures and, importantly, at both higher uranium levels and more extreme temperatures. We therefore report the results of molecular dynamics simulations studying pure and U-doped thoria focussing particularly on the thermal expansivity, bulk structure, heat capacity and ion diffusivity, over a uranium doping range from 1% to 10%, and over a temperature range of 1500 K up to 3600 K.

A. Thermal expansivity

The melting point of thorium oxide is 3663 K—the highest of all oxides. Only a few elements (including tungsten and carbon) and a few compounds (including tantalum carbide) have higher melting points.[20] Computer simulation allows useful predictions to be made, both at operating temperatures and at extreme temperatures approaching the melting point. Furthermore, simulations allow investigations involving a large range of impurity concentrations without the associated cost of a large experimental study. For example, it has been possible to consider pure thoria with very low levels of Uranium ($<$1%) resulting from the decay of Th-233 through to higher levels (10%) of uranium substitution, simulating an actual fuel rod matrix, within a single study.

Our calculations (Table II) suggest that the lattice constant increases by approximately 2% for pure ThO$_2$ and

TABLE I. Potential Parameters for the rigid ion model used in this work.[5]

Interaction type	Buckingham potential		$A \exp(-r/\rho)$–C/r^6
	A /eV	ρ / Å	C/eV Å^6
ThO	1144.6	0.3949	0.00
UO	1055.0	0.3949	0.00
OO	22764.0	0.1490	27.88

TABLE II. Calculated average lattice parameter for each production run simulated temperature over the range of 1500 K and 3600 K, and for Pure ThO$_2$, and 1%, 5%, and 10% U doping. The experimental data are based on the equation a(T) = 5.58 + 4.63 × 10^{-5} T + 4.71 × 10^{-10} T^2 + 2.51 × 10^{-12} T^3 fitted by Yamashita et al. from data measured between room temperature and 1300 K.[23]

| | Lattice parameter/Å | | | | |
| | % uranium content | | | | |
Temperature/K	0	1	5	10	Experiment[23]
1500	5.69	5.69	5.68	5.68	5.66
1800	5.70	5.70	5.69	5.69	5.68
2100	5.71	5.71	5.71	5.70	5.71
2400	5.73	5.73	5.72	5.72	5.73
2700	5.75	5.74	5.74	5.74	5.76
3000	5.76	5.76	5.76	5.75	5.79
3300	5.78	5.78	5.77	5.77	5.83
3600	5.80	5.80	5.79	5.79	5.87

uranium substitutions of 1% and 10% as the temperature increases from 1500 K to 3600 K. Importantly, when the average lattice parameter is plotted against temperature for each concentration of uranium (Figure 1) there is near perfect correlation to a linear model (R^2 > 0.99). There is no significant difference between the gradients or intercepts of the individual plots at the 5% confidence level, suggesting that doping with these levels of uranium will have little or no effect on the system. Experimental studies of pure and doped thoria have generally considered temperatures below 1600 K and dopant and impurity levels of 10% or more. However, where comparison can be made there is good agreement between experiment and our study. For example, the lattice parameter of pure thoria at 1473 K is reported as 5.66 Å[21] which is only 0.5% smaller than the 5.69 Å we calculate at 1500 K and if the atomistic simulation results of Behera and

Deo[22] are extrapolated to the temperature range we have considered, as shown on Figure 1, the results are also in excellent agreement with the results from our model.

Additionally Yamashita et al. proposed a cubic equation that can be used to predict the lattice parameter of thoria, based on their data measured between room temperature and 1300 K.[23] The predictions from this equation are shown in Table II and even at 3600 K the difference between our calculated values and those derived from the experimental data is only 1%.

Previously, the lattice constant of pure urania has been measured experimentally to increase by 2.29% over a temperature range of 300 K and 2000 K,[23-25] and the computational work of Grover et al.,[14,15] compared a range of 16 different urania potentials and predicted the % increase of lattice constant for pure UO$_2$ to be between 2.5% and 3.6% over the temperature range of 50 K–3000 K, depending on the uranium oxide potential used. Significantly, this is around 1% less than for ThO$_2$ studies described above, pointing to superior, or at the very least comparable, thermal expansivity to that observed for urania even at the extreme temperatures considered here.

The thermal expansion of our U/ThO$_2$ systems can be further probed by calculating the average coefficient of linear expansion (defined here as the average fractional change in lattice parameter per temperature change of 1 K at constant pressure). These results are shown in Figure 2, for each uranium concentration over the full temperature range of the study. On inspection, it is clear that the thermal expansivity of pure ThO$_2$ is small having a coefficient of linear expansion of 9.2 × 10^{-6} K^{-1} at 1500 K, increasing by about 4% to 9.6 × 10^{-6} K^{-1} at 3600 K.

Figure 2 also shows that the uranium levels likely to be found in ThO$_2$ fuel rods due the decay of Th-233 will have very little effect on the thermal expansion (on average less
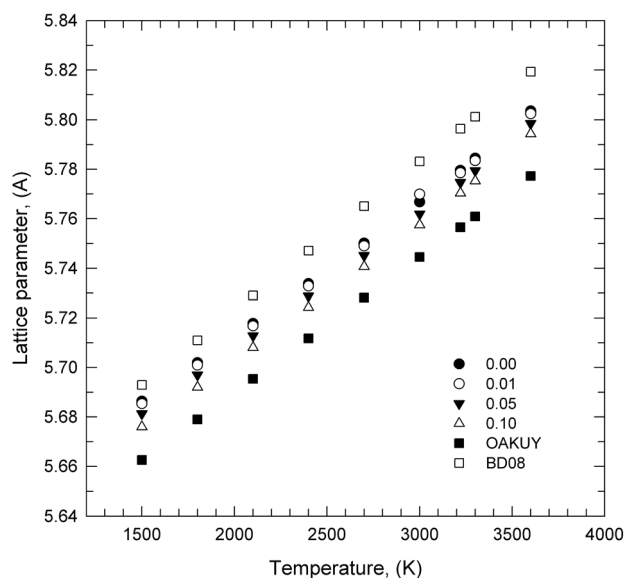

FIG. 1. Plot of lattice parameter against temperature for pure thoria, and systems containing 1%, 5%, and 10% uranium compared to extraplolated published results.[22]
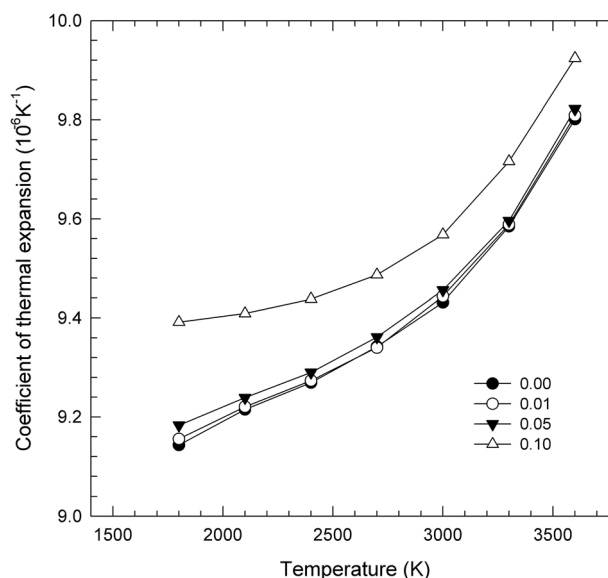

FIG. 2. Coefficient of thermal expansion of uranium/thoria solid solutions as a function of temperature. The higher plot is for the 10% Uranium content; the 3 very similar plots are for the 0% (pure thoria), 1% and 2% Uranium content.

than 0.3% difference between the pure system and the system containing 1% uranium). However, we calculate that the thermal expansion of the sample containing 10% uranium is significantly higher, varying between, 9.4×10^{-6} K^{-1} at 1500 K and 9.9×10^{-6} K^{-1}, an increase of around 2% compared to that of the pure system.

The higher thermal expansion, calculated for the sample containing 10% uranium is still considerably less than that previously determined for urania, and for other oxide nuclear fuels, actinide oxides and other materials used in nuclear applications.[24,26–34] This can be seen in Table III, which shows the values for the coefficient of linear expansion for the other materials varying between 5.0×10^{-6} K^{-1} and 2.8×10^{-5} K^{-1}. At worst the levels of thermal expansion of our systems are comparable to related materials and in most cases are significantly better. We also note that our values are in excellent agreement with previous work, which calculated the average thermal expansion of ThO$_2$ between 298 K and 1473 K to be 9.58×10^6 K^{-1}. In contrast to this a recent density function theory study, making use of linear response lattice dynamics to determine the effect of temperature on the system calculated the thermal expansion coefficient to be an order of magnitude above our calculated values,[35] however, it should be noted that at the heart of this theory is a quasi harmonic approximation that is not valid at temperatures well above the Debye temperature of the material (463 K in the case of ThO$_2$[36]) and also these results not consistent with the published results for thorium oxide and the other actinide oxides shown in Table III.

B. Bulk structure

Having determined how the size of the unit cell varies with temperature it is also important to understand how temperature affects the bulk structure, and particularly the local atomic ordering. It is important that a nuclear fuel material does not undergo a phase change over the temperature range in which it is likely to operate. We have therefore investigated the structure of the pure and doped thoria systems over the full temperature range of the study, by analysing the radial distribution functions (RDF).

In a solid, the RDF consists of a series of sharp peaks, whose separations and heights are characteristic of the lattice structure. A solid phase change, such as zirconia changing to t-ZrO$_2$ from its cubic form, would result in a change in the positions of the sharp peaks in the RDF. As shown in Figure 3, where the Th—O distribution is shown for pure and the 10% U samples as a function of temperature, no significant movement of the peaks or loss of long range order is observed at any of the temperatures or uranium concentrations considered in this study. However, there is a slight decrease (0.2 Å) in the position of the first, nearest neighbour, peak as the temperature increases which is accompanied by a similar sized increase in the position of all the other peaks. This latter effect arises from the thermal expansion of the crystal noted in Sec. III A. The reduction in the average nearest neighbour distance may be due either to the ions becoming increasingly mobile at higher temperatures or to an artefact of the potential model we have used. As expected, there is also a broadening of the peaks as temperature increases, reflecting an increase in lattice disorder, either due to diffusion or simply to the atoms vibrating to a greater extent at their lattice sites.

At first approximation, the structure of the system appears to be independent of uranium content, since for pure thoria (Figure 3(a)), the Th–O distance, as read from the RDF, ranges from 2.28 to 2.38 Å, over the temperature range of 1500–3600 K. Whereas for the system incorporating 10% uranium levels (Figure 3(b)) over the same temperature range, we obtain a Th–O distance which varies over a slightly narrower but still overlapping range of 2.33–2.38 Å. Previously, an extended x-ray absorption fine structure (EXAFS) study of the local structure of solid solutions of Th$_{1-x}$U$_x$O$_2$ and Th$_{1-x}$Pu$_x$O$_2$[37] gave average metal—oxygen distances of 2.424 Å for pure ThO$_2$ and 2.369 Å for pure UO$_2$. At 11% U doping of ThO$_2$ the average metal-oxygen distance was measured to be 2.418 Å. The work for the Th$_{1-x}$Pu$_x$O$_2$ solid solutions gave average metal—oxygen distances of 2.424 Å for pure ThO$_2$ and 2.335 Å for pure PuO$_2$ and 2.419 Å for the system containing 13% Pu. Whilst these quoted values are slightly larger than the values obtained from our simulations they are still within the range of values observed in the molecular dynamics simulations, a point illustrated by the spread of the initial peaks in Figure 3.

A complete set of radial distribution functions is included as supplementary data to this paper.[63] When analysed in conjunction with the results presented here, they support our conclusion that there is no phase change in the material, and indeed they indicate thermodynamic structural stability even at high levels of uranium doping and in extreme temperatures.

An alternative approach to probing any phase change in the system as a function of temperature is to consider the lattice dynamics of the system: In such a simulation, a marked change in the frequencies observed in the phonon density of states indicates that a phase change has occurred, whereas the presence of imaginary frequencies would suggest that the system is in a transitional state.[38] Conventional lattice

TABLE III. Coefficient of linear expansion for a range of oxides from recent experimental and computational studies.

| Material	Coeffient of linear expansion/10^{-6} K^{-1}	Temperature range/K
This work ThO$_2$	9.2–9.8	1500–3600
This work U$_{0.1}$Th$_{0.9}$O$_2$	9.4–9.9	1500–3600
ThO$_2$[27]	9.58	293–1473
ThO$_2$ (simulation)[35]	33–37	298–1500
CeO$_2$[29]	11.6	—
UO$_2$[34]	11.2	—
ZrO$_2$[34]	10–11	—
NpO$_2$[23,26]	9.5–10	300–1200
NpO$_2$ (simulation)[28]	8.0–26	300–2800
AmO$_2$[26,32]	8.0–13	300–1200
AmO$_2$ (simulation)[28]	5.0–15	300–2000
PuO$_2$[24,33]	10–28	250–3000
PuO$_2$ (simulation)[30]	7.0–13	300–3000
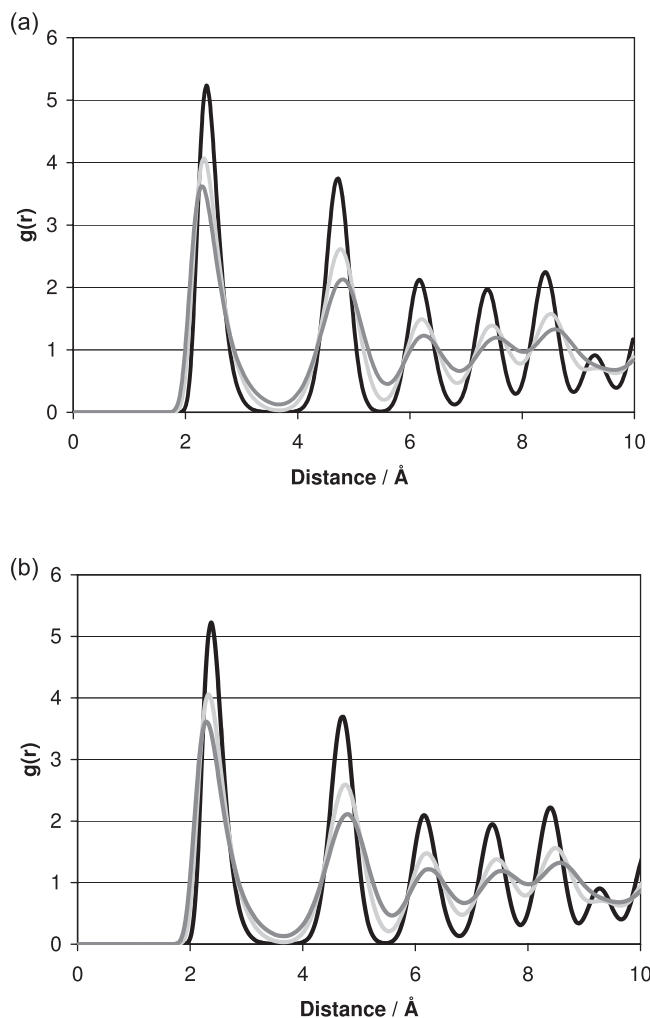
FIG. 3. Th-O radial distribution functions for (a) pure ThO$_2$ (b) ThO$_2$ doped with 10% U. Black line 1500 K, pale grey line 2700 K, and dark grey line 3600 K.

dynamics makes use of a harmonic approximation and has been widely used to study a range of solid materials. However, this approach is not reliable at temperatures well above the Debye temperature of the material (463 K in the case of ThO$_2$[36]). An alternative is to extract the vibrational modes, and hence the density of states, directly from the molecular dynamics trajectories.[39]

We have followed this approach, and the phonon density of states, as a function of temperature, is shown for pure ThO$_2$ in the supplementary material.[63] As expected, and consistent with the RDF presented in Figure 3, the plots show common general features, with additional fine detail present at the lower temperatures. The loss of this detail as the temperature of the system is increased is consistent with the additional motion of the atoms at higher temperatures and as the melting point is approached, but again there is no evidence of a phase change occurring in our simulations.

C. Heat capacity

Physical properties, such as the heat capacity of a nuclear fuel, are required for reactor physics and safety calculations. Indeed, heat capacity controls the fuel temperature

during irradiation and the high temperature heat capacity of a fuel is one of the most important properties for evaluating any change in the fuel's temperature during normal operation and during severe accident.

Previously, UO$_2$ defect calculations have shown that there is a relatively low-energy inter-cation charge transfer process ($2U^{4+} \rightarrow U^{5+} + U^{3+}$),[40] which is responsible for the high temperature specific heat excess in UO$_2$. This is an important phenomenon in possible accident scenarios and is discussed in detail by Stoneham.[41] There is no evidence for such an excitation process in thoria: Creating Th^{5+} would require the removal of a core electron and Th^{3+} is not stable either in the solid or aqueous phases and, as illustrated by the Frost diagram of thorium ions in solution, would be rapidly oxidised to Th^{4+}.[42,43] Therefore, during a severe accident, where pure thoria will be exposed to high temperature and a wide range of oxygen chemical potentials, the melting temperature of ThO$_2$ will not decrease significantly, as might be the case with UO$_2$[44] in similar conditions.

It is, however, important that we investigate the heat capacity of ThO$_2$, and in particular, what the effect of the presence of uranium might have on the heat capacity of the material.

For each of the systems considered in this work, we have plotted the average enthalpy of the simulation against temperature, and since heat capacity can be defined as: $C_p = (\partial H / \partial T)_P$, the instantaneous gradient of such plots represents the heat capacity at that particular temperature. In all cases, we found that these plots were linear and thus that the heat capacity is independent of temperature in the range we have considered. Our calculations give a heat capacity of 310 J kg^{-1} K^{-1} for pure thoria over the full temperature range (1500–3600 K). Since electronic excitations are not taken into account by classical molecular dynamics, one may expect some difference between experimental values and our calculations at the elevated temperature. The result is, however, consistent with that calculated by Lu et al.[35] (306 J kg^{-1} K^{-1} or 81 J mol^{-1} K^{-1}) and also with our calculated values for thorium doped lithium fluorides which fall in the range 400–700 J kg^{-1} K^{-1}, and with previous experiments[45] that estimates a value of 1000 J kg^{-1} K^{-1} at 22% ThF$_4$ composition. Interestingly, previous molecular dynamics (MD) studies[31] of UO$_2$ for temperatures between 400 and 2000 K calculate a heat capacity in the range 50–85 J mol^{-1}K^{-1} (i.e., 185–315 J kg^{-1} K^{-1}) and C_p for UO$_2$[46,47] has been experimentally determined to be in the range 60–100 J mol^{-1}K^{-1} (i.e., 222–370 J kg^{-1} K^{-1}) consistent with our calculated value. This gives us some confidence in the accuracy of our estimate and suggests that thoria has a significantly higher, and therefore more favourable, heat capacity than UO$_2$.

Figure 4 illustrates the effect of uranium substitution, defects, oxygen vacancies and interstitials on the calculated heat capacity of ThO$_2$ and shows that an increase in U^{4+} levels in thoria has little effect on the heat capacity of the material as a whole. Even when 10% of the cation sites are substituted with U^{4+} the change in C_p is not significant at the 5% confidence level. However, when oxygen vacancies and oxygen interstitials are included in the system, the calculations do predict a significant change in the heat capacity. The
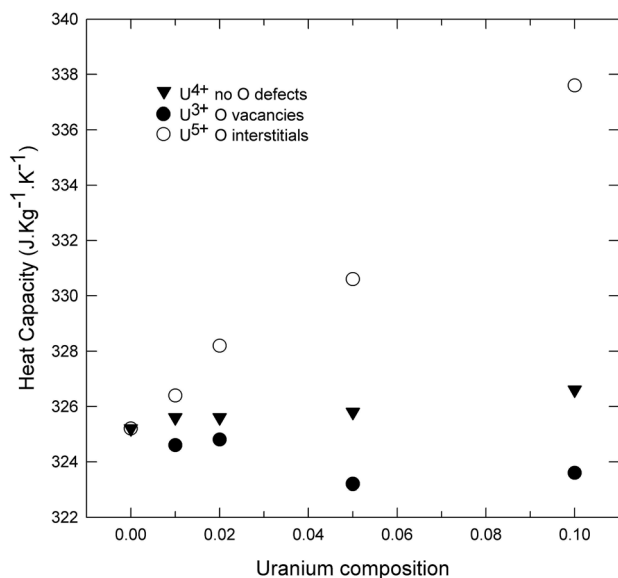
FIG. 4. Plot showing the effect of different Uranium levels and the presence of oxygen vacancies and interstitials on the heat capacity of Thoria. Shaded triangles U^{4+} doped (no oxygen defects), solid circles U^{3+} doped (with oxygen vacancies), open circles U^{5+} doped (with oxygen interstitials).

simulations containing oxygen vacancies show only a small (at most, 2%) drop in heat capacity the magnitude of which does not increase even when high concentrations of vacancies are present. However, as the level of uranium V doping is increased, and hence the number of charge compensating oxygen interstitials increases, the heat capacity also steadily rises.

The predicted small decrease in C_p for increased levels of uranium III and associated oxygen vacancies is a consequence of these defects decreasing the density of the material and increasing the molecular freedom throughout the crystalline lattice. In a similar way, the calculated steady and significant increase in C_p as the levels of uranium V and associated oxygen interstitials increases results from these defects increasing the density whilst correspondingly decreasing the molecular freedom throughout the crystalline lattice. With less molecular freedom, the material will need more heat to cause a change in its temperature.

Our calculations predict uranium IV impurities in the pure thoria crystal have virtually no effect on C_p, even in the most extreme conditions considered. This might be expected as the uranium impurities in the pure crystal will not increase the number of oxygen vacancies or interstitials, so the density of the material and the molecular freedom essentially remains unaltered and, as uranium IV ions are of similar size to thorium, relatively large amounts of uranium can be incorporated into ThO_2 without changing the stability of the material significantly.

D. Diffusion

Related to the discussion of molecular freedom is the ease of which ions can diffuse within the crystal lattice. The diffusion of oxygen in actinide oxide fuels is of considerable importance in the safety management of nuclear fuels. For instance, the inhomogeneity caused by ions moving through

the lattice can lower the melting point and thermal conductivity of the material leading to local burn-up.[48] In addition, the distribution of oxygen ions in the crystal lattice affects the properties of any fission products.[48,49] Such diffusion in reactor fuels is generally found under complex circumstances far from equilibrium. However, in order to understand such complex phenomena, we must first determine the mechanism for oxygen diffusion in more ideal conditions

As the formation of anion Frenkels is known to dominate the defect chemistry of many fluorite materials,[50] it is likely oxygen diffusion will be observed in thoria and the activation energy will be similar to the anion Frenkel, energy, which we calculate to be 3.31 eV/defect, using the same potential parameters to those used in our MD simulations and the Mott-Littleton approach implemented in GULP 3.4,[51,52] which also compares favourably with the values of Lu et al (3.42 eV/defect).[35]

Based on the trajectories of the atoms in our molecular dynamics simulations, it is possible to construct mean square displacement plots for all of our pure and defective thoria systems as a function of temperature (included as supplementary data to this work).[63] If diffusion is occurring in the system then the graph will be linear and the gradient is directly related to the diffusion coefficient at the temperature considered. Plotting the natural logarithm of the diffusion coefficient against inverse temperature should then give a linear correlation (if the system is following Arrhenius behaviour), where the gradient is $-E_a/R$, with E_a being the activation barrier to diffusion and R the ideal gas constant.

Such a plot is shown in Figure 5, where we have only plotted points for which the diffusion coefficient is calculated as being greater than 10^{-10} m^2 s^{-1}, as below this value it is reasonable to assume that no diffusion is taking place. On inspection of Figure 5, it is clear that there is little or no diffusion occurring in systems where the cations and oxygen are present in the correct stoichiometric proportions, with the activation energies being between 3.6 and 3.9 eV (see Table IV). This is within 10% of our calculated value for the
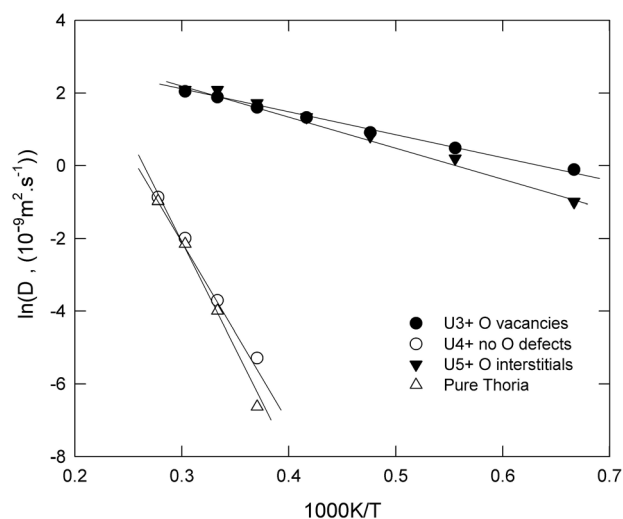

FIG. 5. Arrhenius plots for pure Thoria and for 10% Uranium doping, containing U^{5+} and oxygen interstitials, U^{4+} and no oxygen defects and U^{3+} and containing oxygen vacancies.

TABLE IV. Calculated activation barriers to diffusion as a function of uranium content and oxygen defect concentration in ThO_2.

% U dopant	Activation energy Ea / eV		
	U^{4+}no O defects	U^{3+}O vacancies	U^{5+}O interstitials
0.0	3.8	3.8	3.8
1.0	3.8	1.9	0.7
2.0	3.9	0.5	0.7
5.0	3.9	0.5	0.7
10.0	3.6	0.5	0.7

formation of anion Frenkel defects, illustrating that significant oxygen diffusion is only likely to occur at temperatures well above the standard operating conditions of any nuclear reactor, providing the fuel remains stoichiometrically pure. These predictions are again indicative of the high thermal stability of thorium oxide and compare well with experimental measurements of oxygen diffusion in pure thoria[49] which lists diffusion enthalpies from a variety of experimental studies in the range 220–452 kJ mol^{-1} (2.3–4.7 eV). Previous isolated defect calculations of Colbourn and Mackrodt[53] give values of 215 kJ mol^{-1} (2.2 eV) and 267 kJ mol^{-1} (2.8 eV) for hyperstoichiometric ThO_2 and hypostoichiometric ThO_2, respectively, although it should be noted that as these result from static calculation, temperature is not an explicit part of the model.

The calculated activation energy for oxygen diffusion in UO_2 has ranged between 2.6 eV and 5.9 eV (see Table V). It should be noted that the higher activations energies are reported in studies incorporating temperatures as low as 500 K, below the point where any significant diffusion and Arrhenius behaviour is likely to be observed. Inclusion of such points has the effect of artificially increasing the calculated activation energy. The lower calculated values for activation energy are typically from higher temperature studies or from those which, like this study, have only included simulation where significant diffusion is occurring in the Arrhenius plots. With this in mind it is predicted that at high temperatures the activation energy for oxygen diffusion is approximately 1 eV lower for UO_2 systems compared to similar ThO_2 systems.

When the anions and cations in the system are not present in stoichiometric proportions, our calculations predict that the barrier to diffusion is significantly reduced. For example, when doped with 10% U^{3+} and compensating

TABLE V. Previous calculated activation energies for lattice oxygen diffusion, in UO_2.

	Activation energies for lattice oxygen diffusion in urania/eV
Arima et al.[57,58]	5.7
Yakub et al.[59]	5.9
Basak et al.[60]	4.3
Armira et al.[61]	5.2–5.7
Matzke (Exp.)[62]	2.6
Matzke (Calc.)[62]	2.8

oxygen vacancies, the E_a reduces to 0.5 eV and the activation energy is calculated to be 0.7 eV for a system doped with 10% U^{5+} and the associated proportion of compensating interstitial oxygen.

Again these values compare well to comparable experimental measurements which gives a values of 74 kJ mol^{-1} (0.77 eV).[54–56] Furthermore, our calculated values once again correspond to the calculations of Colbourn and Mackrodt, which give a value of 75 kJ mol^{-1} (0.78 eV) for vacancy migration arising from vacancies introduced from residual trivalent impurities. This effect is well known in other fluorite minerals: For example, yttrium stabilised ZrO_2 is an early example of a fast ion conductor and simulations have shown that addition of various alliovalent ions to cubic ZrO_2 will promote oxygen within the crystal structure.[7] This past work is, however, based on static simulations of isolated defects, whereas we are considering particular concentrations of defects as a function of temperature.

The general result is therefore that there will be more oxygen diffusion in thoria systems that incorporate oxygen vacancies or interstitials and it is this additional disorder in the system that drives the diffusion. This is particularly true for those systems involving oxygen vacancies because, as we have discussed previously, there is more molecular freedom in such systems. An illustration of this additional freedom is provided by the fact that the systems containing oxygen interstitials are almost entirely dominated by Frenkel disorder whereas in systems containing a large concentration of oxygen vacancies, oxygen diffusion is possible through both Schottky and Frenkel based mechanisms thereby increasing the routes though which diffusion can occur, accounting for the predicted reduction in activation barrier to diffusion. This suggests that once a thorium based fuel has been subject to radiation damage and is therefore highly defective significant oxygen diffusion will occur, although this should be no greater than would occur in other nuclear fuels with the fluorite structure.

IV. CONCLUSION

We have used molecular dynamics simulation to help us determine the suitability of thoria as a next generation nuclear fuel. Uranium has been incorporated into the systems at levels comparable with those found in fuel rods arising from the decay of Th-233, and from pre-doping the fuel with fertile U-235. The MD studies were carried out over a temperature range comparable to that occurring in a reactor through to the particularly harsh conditions that might exist in the case of a serious accident.

The simulations have largely confirmed the hypothesis that ThO_2 has favourable thermo-physical properties which are at least directly comparable to those of existing fuels and in many cases superior to those of UO_2.

Our calculations suggest that thoria has very low thermal expansivity, and that adding uranium to the structure has little effect on its expansivity, even at the highest levels considered, i.e., 10%. When the atomic structure of the material is considered by analysing the RDF no structural phase changes are observed even in the most extreme conditions, considered. This is further confirmed by extracting the

vibrational modes from the simulations and calculating the phonon density of states.

Our calculations predict that there is minimal effect on the heat capacity of thorium oxide either as the temperature increases or as U^{4+} ions are substituted into the crystal structure. Similarly, we calculate that the activation energy for oxygen diffusion in pure thoria is 3.8 eV (close to the calculated energy to form a Frenkel defect) and this changes only by 0.2 eV to 3.6 eV when 10% of the cation sites are occupied by uranium ions.

In both cases, the addition of oxygen vacancies and interstitials changes the properties of the system significantly. The energy barrier to diffusion decreases by over 3 eV, at uranium levels of 2% and higher, to levels which can be overcome spontaneously at operational temperatures. The effect is slightly greater (0.2 eV) in the systems containing vacancies as in such systems diffusion based on a Shottky mechanism is also possible.

These calculated material properties reinforce the suitability of thoria as a nuclear fuel. These findings will form the basis of further studies in which we are modelling the effects of radiation damage, from both fission products and the high energy neutrons used to initiate the conversion of Th-232 to Th-233 and the eventual formation of fissile U-233, via the decay of Pa-233.

ACKNOWLEDGMENTS

[1]M. Lung and O. Gremm, Nucl. Eng. Des. **180**, 133–146 (1998).
[2]M. Osaka, M. Koi, S. Takano, Y. Yamane, and T. Misawa, J. Nucl. Sci. Technol. **43**, 367–374 (2006).
[3]M. Born and K. Huang, *Dynamical Theory of Crystal Lattices* (Oxford University Press, Oxford, 1954.).
[4]P. P. Ewald, Ann. Phys. **64**, 253 (1921).
[5]G. V. Lewis and C. R. A. Catlow, J. Phys. C **18**, 1149–1161 (1985).
[6]M. S. Khan, M. S. Islam, and D. R. Bates, J. Mater. Chem **8**, 2299–2307 (1998).
[7]M. Kilo, R. A. Jackson, and G. Borchardt, Philos. Mag. **83**, 3309–3325 (2003).
[8]S. A. Maicaneanu, D. C. Sayle, and G. W. Watson, Chem. Commun. **2001**, 289–290.
[9]T. X. T. Sayle, S. C. Parker, and C. R. A. Catlow, J. Phys. Chem. **98**, 13625–13630 (1994).
[10]E. V. Stefanovich, A. L. Shluger, and C. R. A. Catlow, Phys. Rev. B **49**, 11560–11571 (1994).
[11]G. Balducci, M. S. Islam, J. Kaspar, P. Fornasiero, and M. Graziani, Chem. Mater. **12**, 677–681 (2000).
[12]B. G. Dick and A. W. Overhauser, Phys. Rev.**112**, 90–103 (1958).
[13]P. J. Mitchell and D. Fincham, J. Phys. Condens. Matter **5**, 1031–1038 (1993).
[14]K. Govers, S. Lemehov, M. Hou, and M. Verwerft, J. Nucl. Mater. **366**, 161–177 (2007).
[15]K. Govers, S. Lemehov, M. Hou, and M. Verwerft, J. Nucl. Mater. **376**, 66–77 (2008).
[16]W. Smith and T. R. Forester, J. Mol. Graphics **14**, 136–141 (1996).
[17]W. G. Hoover, Phys. Rev. A **31**, 1695–1697 (1985).
[18]S. Nose, J. Chem. Phys. **81**, 511–519 (1984).
[19]International atomic energy association, "Thorium fuel cycle—Potential benefits and challenges," (2005); available online at: http://www-pub.iaea.org/mtcd/publications/pdf/te_1450_web.pdf.
[20]J. Emsley, *Nature's Building Blocks Hardcover*, 1st ed. (Oxford University Press, 2001).
[21]G. Panneerselvama, M. P. Antony, and T. Vasudevan, Thermochim. Acta **443**, 109–115 (2006).
[22]R. K. Behera and C. S. Deo, J. Phys. Condens. Matter **24**, 215405 (2012).
[23]T. Yamashita, N. Nitani, T. Tsuji, and H. Inagaki, J. Nucl. Mater. **245**, 72–78 (1997).
[24]D. G. Martin, J. Nucl. Mater. **152**, 94–101 (1988).
[25]D. Taylor, Trans. J. Br. Ceram. Soc. **83**, 32–37 (1984).
[26]J. A. Fahey, R. P. Turcotte, and T. D. Chikalla, Inorg. Nucl. Chem. Lett. **10**, 459–465 (1974).
[27]V. Grover and A. K. Tyagi, Ceram. Int. **31**, 769–772 (2005).
[28]K. Kurosaki, M. Imamura, I. Sato, T. Namekawa, M. Uno, and S. Yamanaka, J. Nucl. Sci. Technol. **41**, 827–831 (2004).
[29]M. D. Mathews, B. R. Ambekar, and A. K. Tyagi, J. Nucl. Mater. **280**, 246–249 (2000).
[30]T. Seetawana, T. Khuangthipa, V. Amornkitbamrunga, K. Kurosakia, J. Adachia, M. Katayamaa, A. Charoenphakdeea, and S. Yamanakaa, in *MRS Proceedings* (2007), Vol. 1043, pp. T09–09.
[31]A. K. Sun, *The Nuclear Fuel Cycle* (Back End Technology Development Division, Bhabha Atomic Research Centre, Trombay, Mumbai).
[32]D. Taylor, Trans. J. Br. Ceram. Soc. **84**, 181–188 (1985).
[33]M. Tokar, A. W. Nutt, and T. K. Keenan, Nucl. Technol. **17**, 147–152 (1973).
[34]H. Warlimont and W. Martienssen, *Springer Handbook of Condensed Matter and Materials Data* (Springer, Berlin/Heidelberg, 2005), Vol. 1.
[35]Y. Lu, Y. Yang, and P. Zhang, J. Phys. Condens. Matter **24**, 225801 (2012).
[36]H. Serizawa, Y. Arai, and Y. Suzuki, J. Nucl. Mater. **280**, 99–105 (2000).
[37]S. Hubert, J. Purans, G. Heisbourg, P. Moisy, and N. Dacheux, Inorg. Chem. **45**, 3887–3894 (2006).
[38]M. T. Dove, *Introduction to Lattice Dynamics* (Cambridge University Press, Cambridge), Vol. 2000.
[39]D. J. Cooke, S. C. Parker, and D. J. Osguthorpe, Phys. Rev. B **67**, 134306 (2003).
[40]D. A. Macinnes and C. R. A. Catlow, J. Nucl. Mater. **89**, 354–358 (1980).
[41]A. M. Stoneham, Philos. Trans. R. Soc. London, Ser. A **368**, 3295–3313.
[42]J. Katz, G. Seaborg, and L. Morss, *The Chemistry of the Actinide Elements*, 2nd ed. (Longman, London, 1986).
[43]F. Shriver, P. W. Atkins, and C. H. Langford, *Inorganic Chemistry*, 2 ed. (W. H. Freeman and Co., New York, 1994).
[44]P. Y. Chevalier and E. Fischer, J. Nucl. Mater. **257**, 213–255 (1998).
[45]O. Benes and R. J. M. Konings, J. Fluorine Chem. **130**, 22–29 (2009).
[46]J. K. Fink, J. Nucl. Mater. **279**, 1–18 (2000).
[47]D. Olander, *Fundamental Aspects of Nuclear Reactor Fuel Elements* (US Dept of Energy, 1976).
[48]H. Kleykamp, J. Nucl. Mater. **131**, 221–246 (1985).
[49]G. E. Murch and C. R. A. Catlow, J. Chem. Soc., Faraday Trans. **83**, 1157–1169 (1987).
[50]A. R. West, *Basic Solid State Chemistry*, 2nd ed. (John Wiley and Sons Chichester, 2000).
[51]J. D. Gale and A. L. Rohl, Mol. Simul. **29**, 291–341 (2003).
[52]N. F. Mott and M. J. Littleton, Trans. Faraday Soc. **38**, 485–499 (1938).
[53]E. A. Colbourn and W. C. Mackrodt, J. Nucl. Mater. **118**, 50–59 (1983).
[54]K. Ando and Y. Oishi, J. Nucl. Sci. Technol. **16**, 214–220 (1979).
[55]K. Ando and Y. Oishi, Solid State Ionics **3–4**, 473–476 (1981).
[56]K. Ando, Y. Oishi, and Y. Hidaka, J. Chem. Phys. **65**, 2751–2755 (1976).
[57]T. Arima, K. Idemitsu, Y. Inagaki, Y. Tsujita, M. Kinoshita, and E. Yakub J. Nucl. Mater. **389**, 149–154 (2009).
[58]T. Arima, S. Yamasaki, Y. Inagaki, and K. Idemitsu, J. Alloys Compd. **400**, 43–50 (2005).
[59]E. Yakub, C. Ronchi, and D. Staicu, J. Chem. Phys. **127**, 094508 (2007).
[60]C. B. Basak, A. K. Sengupta, and H. S. Kamath, J. Alloys Compd. **360**, 210–216 (2003).
[61]T. Arima, K. Yoshida, K. Idemitsu, Y. Inagaki, and I. Sato, in *Actinides* (2009), Vol. 9.
[62]H. Matzke, J. Less-Common Met. **121**, 537–564 (1986).
[63]See supplemental material at http://dx.doi.org/10.1063/1.4754430 for mean square displacement plots for all pure and defective thoria systems as a function of temperature.